Robustness of 3D Base-Isolated R.C. Systems with FPS

Robustness of 3D base-isolated R.C. systems with FPS

P. Castaldo[1], G. Mancini[1], B. Palazzo[2]

[1] *Department of Structural, Geotechnical and Building Engineering, Politecnico di Torino, Turin, Italy*

[2] *Department of Civil Engineering, University of Salerno, Salerno, Italy*

ABSTRACT: This study evaluates the seismic robustness of 3D r.c. structures isolated with single-concave friction pendulum system (FPS) devices by computing the seismic reliability of different models related to different malfunction cases of the seismic isolators. Considering the elastic response pseudo-acceleration as the relevant random variable, the input data have been defined by means of the Latin Hypercube Sampling technique in order to develop 3D inelastic time-history analyses. In this way, bivariate structural performance curves at each level of the r.c. structural systems as well as seismic reliability-based design abacuses for the FP devices have been computed and compared in order to evaluate the robustness of the r.c. system considering different failure cases of the FP bearings. Moreover, the seismic robustness is examined by considering both a configuration equipped with beams connecting the substructure columns and a configuration without these connecting beams in order to demonstrate their effectiveness and provide useful design recommendations for base-isolated structural systems equipped with FPS.

KEYWORDS: seismic isolation; friction pendulum devices; seismic robustness; structural performance; connecting beams

1 INTRODUCTION

Over the last years, friction pendulum system (FPS) devices have become more and more an effective technique for the seismic protection of structures and infrastructure (Zayas et al. 1990). Several robustness and probabilistic analyses, structural reliability methods and reliability-based analyses (Chen et al. 2007, Kelly et al. 1987) by estimating the stochastic responses of base-isolated systems under random earthquake excitations as well as reliability-based optimizations of base-isolated structures including uncertainties such as isolator properties and ground motion characteristics (Alhan and Gavin 2005, Zou et al. 2010, Mishra et al. 2013, Zhao and Chen 2013) have been performed. The influence of the FPS properties on the seismic response of base-isolated systems has been presented by (Castaldo and Tubaldi 2015) proposing a nondimensionalization of the motion equations for a two-degree-of-freedom system. Seismic reliability analyses of a reinforce concrete (r.c.) 3D base-isolated system with a lifetime of 50 years and located near L'Aquila site (Italy) have been performed in (Castaldo et al. 2015) highlighting the influence of the bivariate correlation between the response parameters on the structural performance (SP) curves and proposing a seismic reliability-based design method to define the isolator dimensions. In (Castaldo et al. 2016), the life-cycle cost analysis (LCCA) of a r.c. 3D system equipped with FP devices is discussed describing the positive benefits derived from increasing values of the isolation degree. For different structural properties, the seismic reliability-based design approach has been proposed in (Castaldo et al. 2017a) with the scope to provide useful design solutions for the seismic devices. In (Castaldo and Ripani 2016), the optimal friction values of FP isolators for the different soil conditions have been discussed and evaluated. Seismic reliability-based relationships between the strength reduction factors and the displacement ductility demand for base-isolated systems have been presented in (Castaldo et al. 2017b). In addition, the robustness analysis of base-isolated high-rise buildings with friction-type bearings and a robust design optimization of base isolation system have been presented, respectively, in (Takewaki 2008) and (Roy and Chakraborty 2015).

This study evaluates the seismic robustness of a 3D r.c. base-isolated structure equipped with single-concave friction pendulum system (FPS) devices, designed according to NTC08 (NTC 2008) by estimating the seismic reliability in its design life (50 years) of different models related to different malfunction cases of the seismic isolators. For the seismic reliability assessment, the elastic response pseudo-acceleration corresponding to the isolated period is assumed as the relevant random variable, modeled through a Gaussian probability density function (PDF) (NTC 2008). By means of the Latin Hypercube Sampling (LHS) technique (Mckey 1979, Celarec and Dolšek 2013), the input data have been defined for each model and 3D inelastic time-history analyses have been developed. In this way, bivariate structural performance (SP) curves at each level of the r.c. structure as well as seismic reliability-based design (SRBD) abacuses for the FP bearings have been computed and compared in order to evaluate the robustness of the system for the different failure cases considered. Moreover, the seismic robustness of the abovementioned r.c. structure has also been examined by considering both a configuration equipped with r.c. beams connecting the substructure columns and a configuration without these connecting beams in order to demonstrate their effectiveness in improving the seismic robustness.

2 FAILURE CASES AND UNCERTAINTIES FOR THE SEISMIC ROBUSTNESS ASSESSMENT

The seismic robustness assessment of the base-isolated r.c. structure is herein developed in probabilistic terms estimating the seismic reliability in the performance space (Bertero and Bertero 2002) by means of a comparison between the performance objective (PO) curves and the SP curves of the different models representative of the different failure cases of the seismic devices. According to (SEAOC-Vision 2000, CEN 2006, FEMA-274 1997), relationships between the four structural PO levels, expressed in terms of the maximum interstory drift limits for each limit state (*LS*), and the corresponding probabilities exceeding the *LS* thresholds during the lifetime (50 years) of the structural system (Tena-Colunga and Escamilla-Cruz 2007), are presented in Table 1, according to both American (FEMA-356 2000) and Italian sesmic code (NTC 2008) provisions, respectively, for a fixed-base (FB) and a base-isolated (BI) structure. In this study, mono/bi-variate interstory drift δ for the sub/super-structure and mono/bi-variate relative displacement u for the FPS, respectively, are assumed as the engineering demand parameters (EDPs).

As for the structural systems, a four-story symmetric r.c. 3D frame building, shown in Figure 1, with a lifetime of 50 years and located in L'Aquila site (geographic coordinates 41°58'25'' N, 13°24'00" E, Italy), analysed in similar studies (Castaldo et al. 2015,2016, Almazàn and De la Llera 2003), has been considered in this work. Three (4^{th}, 3^{rd}, 2^{nd} stories) and one (1^{st} story) levels and the FPS isolation level compose the base-isolated r.c. structure. As already mentioned and also shown in Figure 1, both a configuration equipped with beams connecting the substructure columns and a configuration without these connecting beams are considered. Assuming a radius of curvature R=1.5 m and a design sliding friction coefficient equal to μ=3% (Castaldo et al. 2017b) for the FPS, the base-isolated r.c. structure has been designed in compliance with the life safety *LS* (Castaldo et al. 2017b, Kilar and Koren 2009, Naeim and Kelly 1999), considering a soil type B and a behavior factor q=1.5 (NTC 2008). A post-yield stiffness ratio higher than 3% characterises the superstructure non-linear response along each direction. More details may be found in (Castaldo et al. 2015,2016).

Note that, in the design assumptions of the seismic hazard corresponding to L'Aquila site (Italy) and of the sliding friction coefficient μ=3%, with reference to the both structural configurations, all the design and construction recommendations provided from both (SEAOC-Vision 2000) and (FEMA-356 2000), related to the life safety *LS*, are respected as well as, regarding "*LS1*" and "*LS2*", the stiffness of the frames assures the respect of the more restrictive performance requirements for BI structures (NTC 2008, FEMA-356 2000) (Table 1) at each story, especially, in the configuration with the connecting beams (Figure 1(a)). Moreover, note also that the lack of the connecting beams, having section dimensions 0.30 × 0.30 m (Figure 1) and modelled as elastic axial bracing elements, at the substructure level does not modify the construction and design details of the super/sub-structure elements under the abovementioned design assumptions (μ=3%). A FEM model for each structural configuration has been defined in SAP2000 (SAP2000 2002) as shown in Figure 1. From the eigenvalue analyses developed on the BI and FB structural system, the first period of the FB structure is equal to T_{fb} = 0.58 s, the first period of the BI system T_{is} is 2.58 s leading to a value of the isolation degree I_d higher than 3 (NTC 2008, FEMA-356 2000). Within a Rayleigh damping model, imposing a damping factor ξ_{is}= 2% on the first two modes of the 3D BI system (Alhan and Gavin 2005, Castaldo et al. 2015,2016, Almazàn and De la Llera 2003), mass proportional α and stiffness proportional β coefficients have been set equal to 0.0244 and 0.0041, respectively. In the FEM model, with reference to the non-linear behavior of each FPS device, the force is expressed as (Castaldo et al. 2015,2016, Naeim and Kelly 1999):

$$F = \mu W \operatorname{sgn}(\dot{u}) + \frac{W}{R} u \tag{1}$$

in which, *sgn* denotes the signum function of the sliding velocity $\dot{u}$. In particular, the non-linear dependence of the friction coefficient μ on the sliding velocity of each frictional device, as described in (Castaldo et al. 2015,2016,2017b), has been modelled as (Constantinou et al. 1990,2007, Mokha 1990):

$$\mu = f_{\max} - \left(f_{\max} - f_{\min}\right)\exp\left(-\alpha\dot{u}\right) \tag{2}$$

where f_{max} and f_{min} represent, respectively, the sliding friction coefficients at large and nearly zero sliding velocities. The rate parameter "*a"* is set equal to 50 sec/m (Constantinou et al. 1990, 2007). In order to take into account the stick-slip phenomenon, the abovementioned velocity-dependent equation can be modified as follows (Fagà et al. 2016):

$$\mu = f_{\max} - \left(f_{\max} - f_{rev}\right)\exp\left(-\alpha\dot{u}\right) \tag{3}$$

where f_{max} and f_{rev} represent the reference friction coefficient and the friction coefficient at motion reversals (stick-slip phases) (Fagà et al. 2016), respectively.

Regarding the inelastic behaviour of the r.c. structural members, a lumped plasticity approach has been adopted for each structural configuration (FEMA-356 2000) considering the interaction between the axial force and the bending moments (P-M_y-M_x) and the interaction between the bending moments (M_y-M_x) for the plastic hinges of the columns and of the beams, respectively.

With reference to the failure scenarios for the seismic robustness assessment, for each structural configuration, different models related to different malfunction cases of the FP devices are herein considered in order to evaluate the consequential damage to the structural system. In particular, different deterministic values of the sliding friction coefficient are assumed in order to take into account both the stick-slip phenomenon and the potential failure behaviour of an isolator, characterised by a very high friction coefficient. In Table 2, all the details related to the different models are reported according to Eq. (3) and to the numbering of both the devices and joints illustrated in Figure 1. From the models reported in Table 2, note that a very influencing difference exists between an internal and corner device: the internal isolator is subjected to an almost double weight with respect to the corner device so that if a malfunction affects an internal isolator, a higher eccentricity between the forces of the isolation level, of the superstructure and of the substructure occurs.

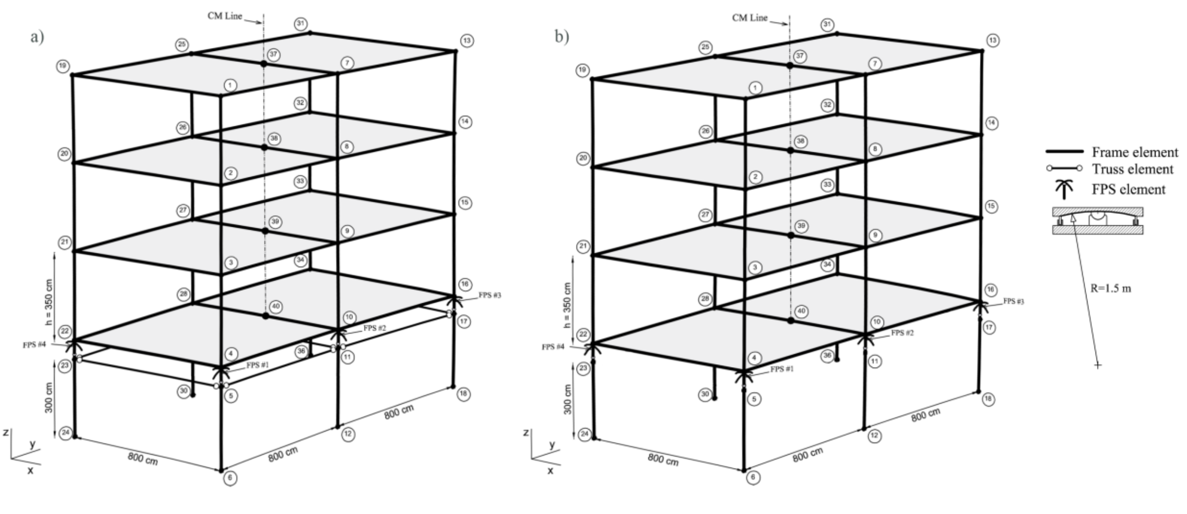

Figure 1. Base-isolated structure configurations with(a) and without(b) the beams connecting the substructure columns.

Finally, regarding the uncertainties, the elastic response pseudo-acceleration corresponding to the isolated structural period with an inherent damping factor of 2% is assumed as the main random variable, modelled by a Gaussian PDF (Castaldo et al. 2016, Cornell 1968, Luco and Cornell 2007), relevant to the structural performance (Castaldo et al. 2016). More details about the abovementoned Gaussian PDF, the sampling procedure and the registration selection criterion are described in (Castaldo et al. 2015, Castaldo 2018a,b,c,d,e,f

Castaldo et al. 2013). Within the 3D inelastic simulations, each earthquake event has been considered with its corresponding three components. The details of the real registrations, selected from the European Strong-Motion Database (ESMD), may be found in (Castaldo et al. 2015) and in (Castaldo et al. 2016).

Table 1. Limit states in terms of maximum Interstory Drift Indices (IDI) and reliability indices in 50 years for fixed-base and base-isolated systems (Castaldo et al. 2017b, Tena-Colunga and Escamilla-Cruz 2007, FEMA-356 2000).

Limit State	**Damage**	**FB structure IDI (%)**	β	P_f	**BI structure IDI (%) (NTC 08)**	**BI structure IDI (%) (FEMA-274)**
LS1	Slight	0 < IDI < 0.3	0	$5.0 \cdot 10^{-1}$	0 < IDI < 0.2	0 < IDI < 0.1
LS2	Moderate	0.3 < IDI < 0.6	1	$1.6 \cdot 10^{-1}$	0.2 < IDI < 0.4	0.1 < IDI < 0.2
LS3	Heavy	0.6 < IDI < 1.5	2	$2.2 \cdot 10^{-2}$	0.4 < IDI < 1.0	0.2 < IDI < 0.5
LS4	Collapsed	IDI > 2	3	$1.5 \cdot 10^{-3}$	IDI > 1.3	IDI > 0.7

Table 2. Friction coefficient properties for the different models.

Models	**FPS#1 Properties (joint-5)**	**FPS#2 Properties (joint-11)**	**FPS#3 Properties (joint-17)**	**FPS#4 Properties (joint-23)**	**FPS#5 Properties (joint-29)**	**FPS#6 Properties (joint-35)**
Model 1	f_{max}=0.03 f_{rev}=0.03	f_{max}=0.03 f_{rev}=0.03	f_{max}=0.03 f_{rev}=0.03	f_{max}=0.03 f_{rev}=0.03	f_{max}=0.03 f_{rev}=0.03	f_{max}=0.03 f_{rev}=0.03
Model 2	f_{max}=0.03 f_{rev}=0.07	f_{max}=0.03 f_{rev}=0.07	f_{max}=0.03 f_{rev}=0.07	f_{max}=0.03 f_{rev}=0.07	f_{max}=0.03 f_{rev}=0.07	f_{max}=0.03 f_{rev}=0.07
Model 3	f_{max}=0.03 f_{rev}=0.07	f_{max}=0.03 f_{rev}=0.07	f_{max}=0.03 f_{rev}=0.07	f_{max}=0.03 f_{rev}=0.07	f_{max}=0.03 f_{rev}=0.07	f_{max}=0.03 f_{rev}=0.20
Model 4	f_{max}=0.03 f_{rev}=0.07	f_{max}=0.03 f_{rev}=0.07	f_{max}=0.03 f_{rev}=0.07	f_{max}=0.03 f_{rev}=0.07	f_{max}=0.03 f_{rev}=0.20	f_{max}=0.03 f_{rev}=0.07
Model 5	f_{max}=0.03 f_{rev}=0.07	f_{max}=0.03 f_{rev}=0.07	f_{max}=0.03 f_{rev}=0.07	f_{max}=0.03 f_{rev}=0.07	f_{max}=0.03 f_{rev}=0.07	f_{max}=0.03 f_{rev}=0.40
Model 6	f_{max}=0.03 f_{rev}=0.07	f_{max}=0.03 f_{rev}=0.07	f_{max}=0.03 f_{rev}=0.07	f_{max}=0.03 f_{rev}=0.07	f_{max}=0.03 f_{rev}=0.40	f_{max}=0.03 f_{rev}=0.07

3 SEISMIC RELIABILITY-BASED ROBUSTNESS ASSESSMENT

In order to estimate the seismic reliability-based robustness of the super/sub-structure and of the FP devices in the different failure cases, several inelastic dynamic simulations have been performed in SAP2000 (SAP2000 2002) for each corresponding structural model and for the both structural system configurations taking into account the seismic uncertainty. Indeed, for each numerical analysis, the peak interstory drifts, δ_x and δ_y, at each story of the super/sub-structure as well as the extreme relative displacements, u_x and u_y, of the FP device level have been computed along x and y directions, respectively. These EDPs have been fitted by means of bi/mono-variate lognormal distributions (Castaldo et al. 2016,2016,2017a,b) estimating, through the maximum likelihood estimation technique, the mean and standard deviation in both directions (x and y directions).

Figures 2-3 show the lognormal monovariate cumulative distribution functions (CDFs) in each direction for all the models and for the two structural configurations at the 4thlevel of the superstructure and at joint (# 29) of the substructure, respectively. At the superstructure along the both directions, Models 6 and 4 lead to the worst effects due to the high eccentricity between the forces of the isolation level and of the superstructure. Regarding the substructure, a failure case related to a substructure column causes the highest monovariate exceeding probabilities on the substructure column itself in both directions (Models 6 and 4 on joint-29) (Figure 3). The connecting beams allow to strongly reduce the failure probabilities at the substructure level thanks to an increase of the structural redundancy among all the substructure columns.

As demonstrated in (Castaldo et al. 2015,2016), the seismic reliability assessment has been carried out in terms of bivariate exceeding probabilities. The JPDFs corresponding to joint-29 of the substructure are shown in Figure 4 as contour lines for Model 6. The statistical parameters of the JPDFs corresponding to the substructure columns strongly increase in the case without the connecting beams as illustrated in Figure 4(b).

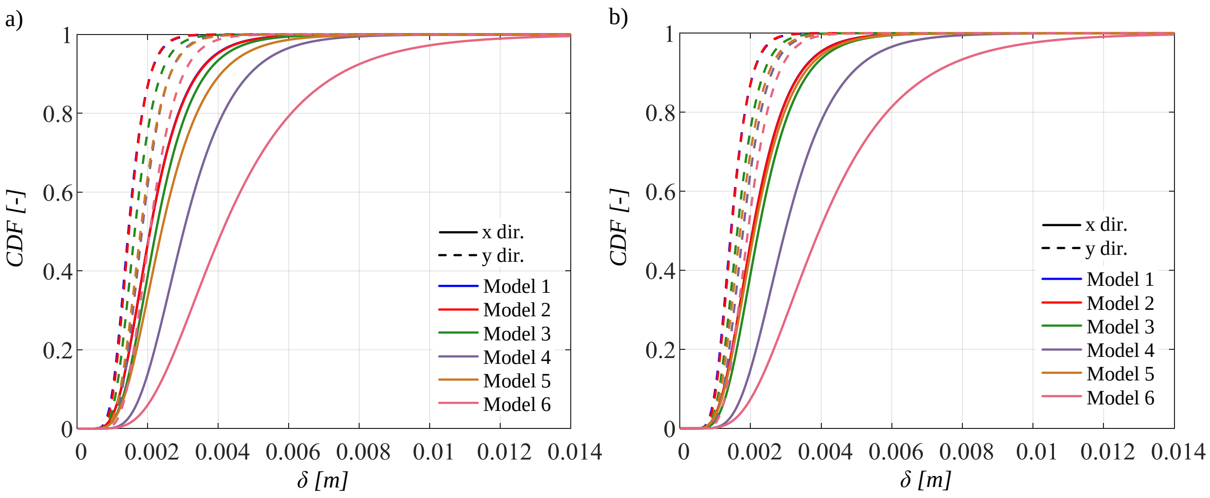

Figure 2. Lognormal monovariate PDFs at the 4th story: structure with (a) and without (b) the connecting beams.

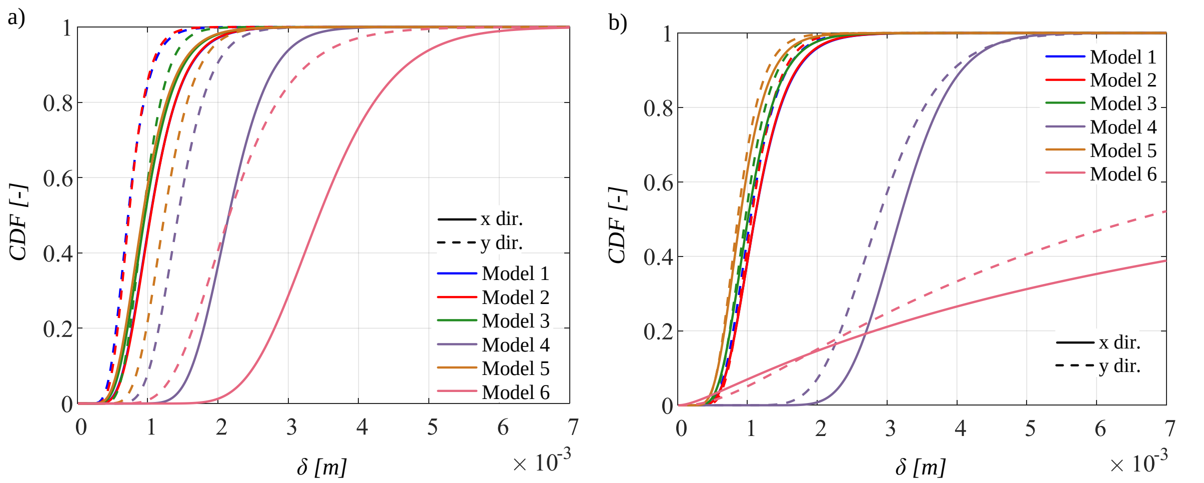

Figure 3. Lognormal monovariate PDFs at the substructure-joint 29: structure with (a) and without (b) the connecting beams.

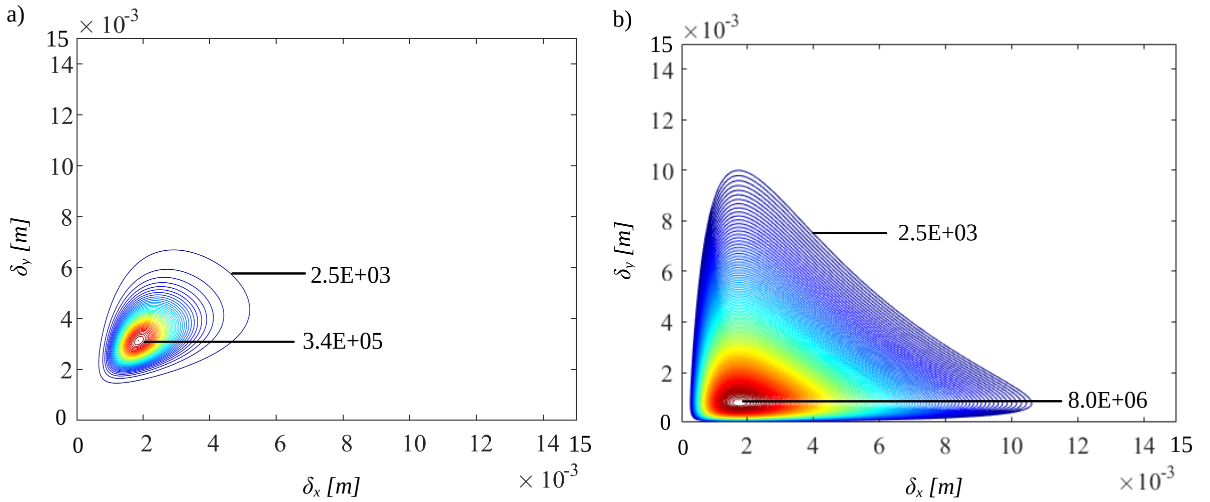

Figure 4. Contour lines of lognormal bivariate PDFs at the substructure-joint 29, related to Model 6, for configuration with (a) and without (b) connecting beams.

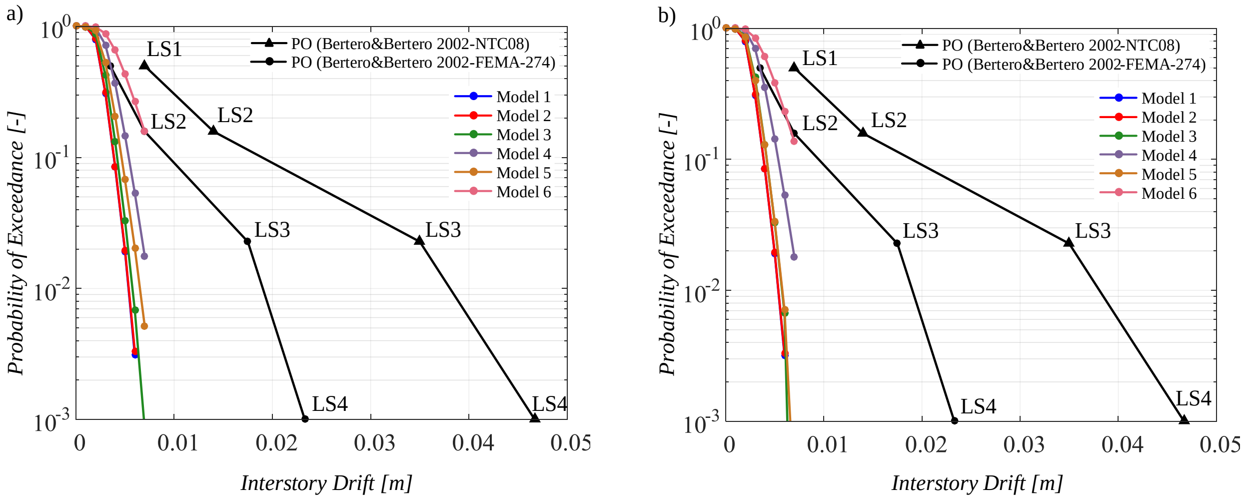

Figure 5. Exceeding bivariate probabilities at the 4th story, related to configuration with (a) and without (b) the connecting beams.

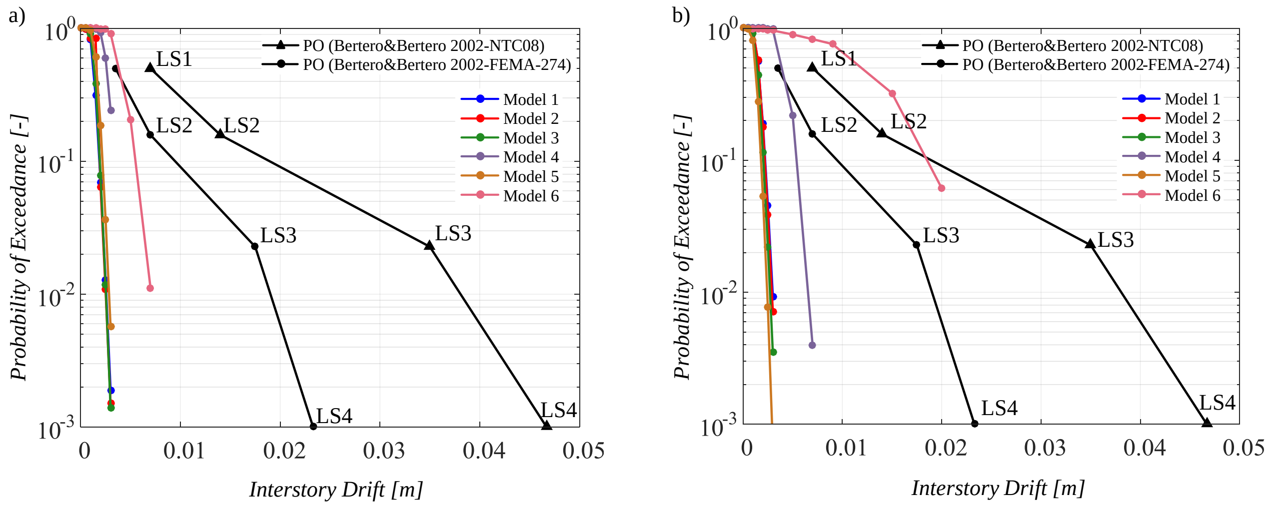

Figure 6. Exceeding bivariate probabilities at the substructure-joint 29, related to configuration with (a) and without (b) the connecting beams.

Next, defining several *LS* functions as bi-dimensional domains on the bi-directional interstory drifts or displacements (bi-dimensional performance objectives POs), the bivariate seismic reliability of the 3D r.c. system has been estimated. Specifically, the no-exceeding bivariate probabilities have been evaluated as follows: for each JPDF, related to each model, configuration and story, the volume delimited by the cylinder representative of the corresponding bi-dimensional *LS* domain, expressed in terms of IDs for the super/substructure and of relative displacements for the FP devices, has been numerically computed. After that, the bivariate exceeding probabilities (bivariate CCDFs), have been numerically calculated as the complementary values of the bivariate no-exceeding probabilities. Figure 5-6 show, in the performance space in logarithmic scale, the bivariate SP curves of the 4th level (superstructure) and of the joint-29 at 1st level (substructure), numerically computed for the different models and configurations, compared to the PO curves according to the both FEMA-274 and NTC08 provisions, as previously discussed. From the comparison, it is possible to evaluate the (bivariate) seismic reliability-based robustness of the overall system and observe that, for the both configurations, the stick-slip phenomenon and malfunction of the FP devices slightly decrease the bivariate seismic reliability of the superstructure, as shown in Fig. 5.

With reference to the substructure, joint-29 (Figure 6), Models 4 and 6, similarly to the monovariate assessment, lead to the lowest seismic reliability values so that the both *LS1* and *LS2*, related to the both PO curves defined according, respectively, to FEMA-274 and NTC08 provisions, are violated in the case without the connecting beams. Moreover, *LS3* and *LS4* according to FEMA-274 are also violated in the case without the connecting beams with the consequence that a severe damage to the substructure can occur. This also means that if a malfunction of an internal device causes a friction coefficient higher than 40%, the substructure column can really collapse leading to a disproportioned damage to the overall system in the case without the connecting beams.

Finally, Figure 7 illustrates the bivariate SP curves of the FP devices showing that these results can be useful for their design (i.e. radius in plan *r*) within the approach of the seismic reliability-based design (SRBD) (Castaldo et al. 2015,2016,2017a,b). The R-square coefficients are higher than 0.97 for all the proposed regressions demonstrating their effectiveness. Form these regression curves, it is possible to observe that with the aim to achieve a given (bivariate) exceeding P_f, a higher radius in plan *r* is necessary in the case of a malfunction of a corner device. In particular, a failure probability of $P_f = 1.5 \cdot 10^{-3}$ (in 50 years) requires a radius in plan *r* ranging from 0.30 m to 0.40 m.

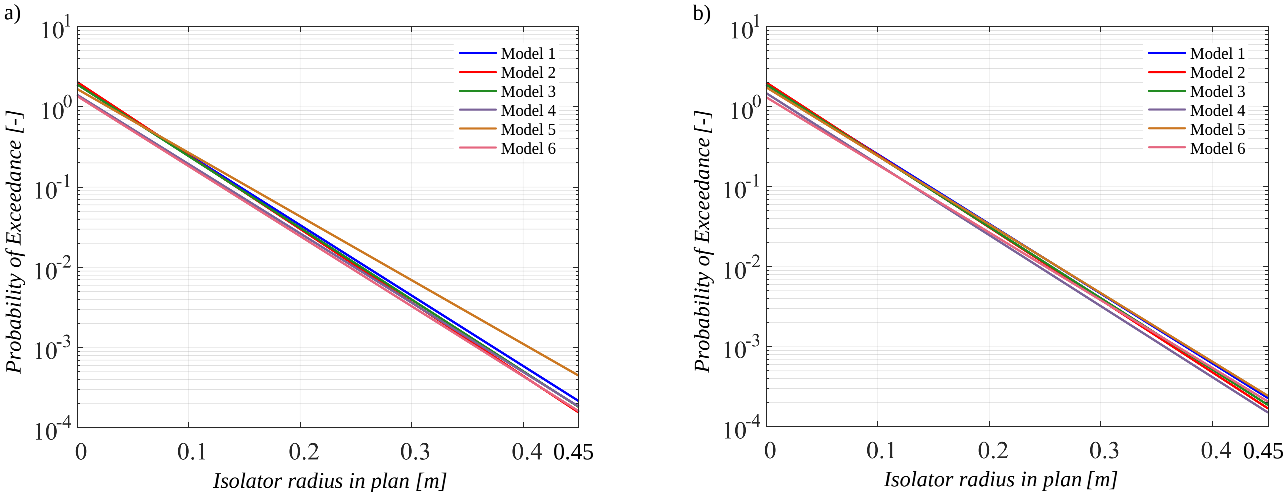

Figure 7. Exceeding bivariate probabilities at the FP devices, related to configuration with (a) and without (b) the connecting beams.

4 CONCLUSIONS

The scope of this work is to estimate the seismic robustness of an ordinary 3D r.c. structure equipped with FP devices, in probabilistic terms, highlighting the importance of the connecting beams at the substructure story. In particular, different models related to different failure cases of the FP devices are presented and, assuming a lifetime of 50 years and L'Aquila (Italy) as reference site, the earthquake main characteristics are assumed as the relevant random variables. The seismic reliability-based results of the 3D r.c. structural system highlight that the presence of the connecting beams strongly improves the seismic reliability and robustness of the substructure by means of an increase of the structural redundancy allowing the respect of the limit states provided by both NTC08 and FEMA-274 provisions. Moreover, it is also possible to declare that the connecting beams at the substructure level mainly increase the seismic robustness of the substructure without negatively modifying the seismic reliability of the superstructure and isolation level by means of an increase of the structural redundancy for a malfunction of a device. This improvement in terms of the seismic reliability and robustness of the substructure also leads to an increase of the foundation safety. Therefore, the diaphragm floor at the superstructure as well as the connecting beams at the substructure allow to avoid a damage disproportionate to the original cause and, so, can represent very useful design solutions and recommendations aimed at improving the robustness of base-isolated systems equipped with FPS in the case of a real malfunction of a seismic frictional device.

REFERENCES

Alhan C, Gavin HP (2005). Reliability of base isolation for the protection of critical equipment from earthquake hazards. *Engineering Structures*, 27:1435-1449.

Almazàn JL, De la Llera JC (2003). Physical model for dynamic analysis of structures with FPS isolators. *Earthquake Engineering and Structural Dynamics*, 32:1157–1184 (DOI: 10.1002/eqe.266).

Almazàn JL, De la Llera JC (2003). Physical model for dynamic analysis of structures with FPS isolators. *Earthquake Engineering and Structural Dynamics*, 32:1157–1184 (DOI: 10.1002/eqe.266).

Bertero RD, Bertero VV (2002). Performance-based seismic engineering: the need for a reliable conceptual comprehensive approach. *Earthquake Engineering and Structural Dynamics*, 31:627–652 (DOI: 10.1002/eqe.146).

Building Seismic Safety Council (1997). NEHRP commentary on the guidelines for the seismic rehabilitation of buildings. Provisions (FEMA-274). Washington, DC.

Castaldo P, Amendola G, Palazzo B (2017a). Seismic fragility and reliability of structures isolated by friction pendulum devices: seismic reliability-based design (SRBD), *Earthquake Engineering and Structural Dynamics*, 46(3):425–446, DOI: 10.1002/eqe.2798.

Castaldo P, Palazzo B, Della Vecchia P (2015). Seismic reliability of base-isolated structures with friction pendulum bearings. *Engineering Structures*, 95:80-93.

Castaldo P, Palazzo B, Della Vecchia P (2016). Life-cycle cost and seismic reliability analysis of 3D systems equipped with FPS for different isolation degrees, *Engineering Structures*, 125:349–363..

Castaldo P, Palazzo B, Ferrentino T (2017b). Seismic reliability-based ductility demand evaluation for inelastic base-isolated structures with friction pendulum devices, *Earthquake Engineering and Structural Dynamics*, 46(8): 1245-1266.

Castaldo P, Ripani M (2016). Optimal design of friction pendulum system properties for isolated structures considering different soil conditions. *Soil Dynamics and Earthquake Engineering*, 90:74–87..

Castaldo P, Tubaldi E (2015). Influence of FPS bearing properties on the seismic performance of base-isolated structures. *Earthquake Engineering and Structural Dynamics*, 44(15):2817–2836.

Castaldo, P., Calvello, M., Palazzo, B. 2013 Probabilistic analysis of excavation-induced damages to existing structures, *Computers and Geotechnics*, 53:17-30.

Castaldo, P., Gino, D., Bertagnoli, G., Mancini, G. 2018a Partial safety factor for resistance model uncertainties in 2D non-linear finite element analysis of reinforced concrete structures, *Engineering Structures*, 176: 746-762

Castaldo, P., Gino, D., Carbone, V.I., Mancini, G. 2018b Framework for definition of design formulations from empirical and semi-empirical resistance models, *Structural Concrete*, 19(4): 980-987.

Castaldo, P., Jalayer, F., Palazzo, B. 2018c Probabilistic assessment of groundwater leakage in diaphragm wall joints for deep excavations, *Tunnelling and Underground Space Technology*, 71: 531-543.

Castaldo, P., Mancini, G., Palazzo, B. (2018d) Seismic reliability-based robustness assessment of three-dimensional reinforced concrete systems equipped with single-concave sliding devices, *Engineering Structures*, 163: 373-387.

Castaldo, P., Palazzo, B., Alfano, G., Palumbo, M.F. 2018e Seismic reliability-based ductility demand for hardening and softening structures isolated by friction pendulum bearings, *Structural Control and Health Monitoring*, 25(11),e2256.

Castaldo, P., Ripani, M., Lo Priore, R. 2018f Influence of soil conditions on the optimal sliding friction coefficient for isolated bridges, *Soil Dynamics and Earthquake Engineering*, 111: 131-148.

Celarec D, Dolšek M (2013). The impact of modelling uncertainties on the seismic performance assessment of reinforced concrete frame buildings. *Engineering Structures*, 52:340–354.

CEN (2006). European Committee for Standardization. Eurocode 0: Basis of Structural Design. Final draft. Brussels.

Chen J, Liu W, Peng Y, Li J (2007). Stochastic seismic response and reliability analysis of base-isolated structures. *Journal of Earthquake Engineerin*g, 11:903-924.

Constantinou MC, Mokha A, Reinhorn AM (1990). Teflon Bearings in Base Isolation. II: Modeling. *J. Struct. Eng.*, 116(2):455-474.

Constantinou MC, Whittaker AS, Kalpakidis Y, Fenz DM, Warn GP (2007). Performance of Seismic Isolation Hardware Under Service and Seismic Loading. Technical Report MCEER-07-0012.

Cornell CA (1968). Engineering seismic risk analysis. *Bulletin of the Seismological Society of America*, 58(5):1583–1606.

ESMD http://www.isesd.hi.is/

Fagà E, Ceresa P, Nascimbene R, Moratti M, Pavese A (2016). Modelling curved surface sliding bearings with bilinear constitutive law: effects on the response of seismically isolated buildings, *Mater Struct*, 49: 2179. doi:10.1617/s11527-015-0642-2.

FEMA-356 (2000). Prestandard and Commentary for the Seismic Rehabilitation of Buildings. Federal Emergency Management Agency: Washington, DC.

Kelly J, Leitmann MG, Soldatos AG (1987). Robust Control of Base-Isolated Structures under Earthquake Excitation. *Journal of Optimization Theory and Applications*, 53(2):159–180.

Kilar V, Koren D (2009). Seismic behaviour of asymmetric base isolated structures with various distributions of isolators. *Eng Struct*, 31:910-921.

Luco N, Cornell CA (2007). Structure-specific scalar intensity measures for near-source and ordinary earthquake ground motions. *Earthquake Spectra*, 23(2):357-92.

Mckey MD, Conover WJ, Beckman RJ (1979). A comparison of three methods for selecting values of input variables in the analysis from a computer code. *Technometrics*, 21:239-45.

Mishra SK, Roy BK, Chakraborty S (2013). Reliability-based-design-optimization of base isolated buildings considering stochastic system parameters subjected to random earthquakes. *International Journal of Mechanical Sciences*, 75:123-133.

Mokha A, Constantinou MC, Reinhorn AM (1990). Teflon Bearings in Base Isolation. I: Testing. *J. Struct. Eng.*, 116(2):438-454.

Naeim F, Kelly JM (1999). Design of Seismic Isolated Structures: From Theory to Practice. John Wiley & Sons, Inc..

NTC08 (2008). Norme tecniche per le costruzioni. Gazzetta Ufficiale del 04.02.08, DM 14.01.08, Ministero delle Infrastrutture.

Roy BK, Chakraborty S (2015). Robust optimum design of base isolation system in seismic vibration control of structures under random system parameters. *Structural Safety*, 55: 49–59.

SAP 2000 (2002). Computers and Structures Inc.: Berkley, CA.

SEAOC-Vision 2000 Committee (1995). Vision 2000-a framework for performance-based earthquake engineering, vol.1. Sacramento (CA): Structural Engineers Association of California.

Takewaki I (2008). Robustness of base-isolated high-rise buildings under code-specified ground motions. *Tall and Special Building*, 17(2): 257–271.

Tena-Colunga A, Escamilla-Cruz JL (2007). Torsional amplifications in asymmetric base-isolated structures. *Engineering Structures*, 29(2), 237-47.

Zayas VA, Low SS, Mahin SA (1990). A simple pendulum technique for achieving seismic isolation. *Earthquake Spectra*, 6:317–33.

Zhao C, Chen J (2013). Numerical simulation and investigation of the base isolated NPPC building under three-directional seismic loading. *Nuclear Engineering and Design*, 265:484-496.

Zou XK, Wang Q, Li G, Chan CM (2010). Integrated reliability-based seismic drift design optimization of base-isolated concrete buildings. *Journal of Structural Engineering*, 136:1282-1295.